



HHS Public Access

Author manuscript

Sci Transl Med. Author manuscript; available in PMC 2016 April 08.

Published in final edited form as:

Sci Transl Med. 2015 October 21; 7(310): 310ra168. doi:10.1126/scitranslmed.aaa5937.

Ultrasound-mediated gastrointestinal drug delivery

Carl M. Schoellhammer^{1,2}, Avi Schroeder^{1,2,3}, Ruby Maa¹, Gregory Yves Lauwers⁴, Albert Swiston^{1,*}, Michael Zervas⁵, Ross Barman², Angela M. DiCiccio², William R. Brugge⁶, Daniel G. Anderson^{1,2,7,8}, Daniel Blankschtein^{1,†}, Robert Langer^{1,2,7,8,†}, and Giovanni Traverso^{1,2,6,†}

¹Department of Chemical Engineering, Massachusetts Institute of Technology, Cambridge, MA 02139, USA

²The David H. Koch Institute for Integrative Cancer Research, Massachusetts Institute of Technology, Cambridge, MA 02139, USA

³Faculty of Chemical Engineering, Technion—Israel Institute of Technology, Haifa 32000, Israel

⁴Department of Pathology, Massachusetts General Hospital, Harvard Medical School, Boston, MA, 02114, USA

⁵Department of Mechanical Engineering, Massachusetts Institute of Technology, Cambridge, MA 02139, USA

⁶Division of Gastroenterology, Massachusetts General Hospital, Harvard Medical School, Boston, MA 02114, USA

⁷Institute for Medical Engineering and Science, Massachusetts Institute of Technology, Cambridge, MA 02139, USA

⁸Harvard-MIT Division of Health Sciences and Technology, Massachusetts Institute of Technology, Cambridge, MA 02139, USA

Abstract

There is a significant clinical need for rapid and efficient delivery of drugs directly to the site of diseased tissues for the treatment of gastrointestinal (GI) pathologies, in particular, Crohn's and

[†]Corresponding author. dblank@mit.edu (D.B.); rlanger@mit.edu (R.L.); ctraverso@partners.org (G.T.).

*Present address: Bioengineering Systems and Technologies Group, Massachusetts Institute of Technology Lincoln Laboratory, Lexington, MA 02420, USA.

SUPPLEMENTARY MATERIALS

www.sciencetranslationalmedicine.org/cgi/content/full/7/310/310ra168/DC1

Supplementary Methods

References (33–40)

Author contributions: C.M.S., W.R.B., D.B., R.L., and G.T. conceived and designed the research. C.M.S., A.Schroeder, R.M., G.Y.L., A.Swiston, M.Z., R.B., A.M.D., and G.T. performed the ex vivo experiments. A.M.D. performed the NMR experiments. C.M.S., R.M., R.B., and G.T. performed the in vivo pig experiments. C.M.S., A.Swiston, M.Z., and G.T. performed the acoustic detection experiments in pigs. C.M.S., R.B., and G.T. performed the in vivo mouse experiments. G.Y.L. analyzed and scored the histology. C.M.S. and G.T. performed the statistical analysis. C.M.S., A.Swiston, M.Z., A.M.D., D.G.A., D.B., R.L., and G.T. analyzed the data and wrote the manuscript.

Competing interests: The authors declare U.S. Provisional Patent application no. 62/144,842 filed on 8 April 2015 covering the technologies described.

Data and materials availability: All data for this study are presented here, and all materials are available.

ulcerative colitis. However, complex therapeutic molecules cannot easily be delivered through the GI tract because of physiologic and structural barriers. We report the use of ultrasound as a modality for enhanced drug delivery to the GI tract, with an emphasis on rectal delivery. Ultrasound increased the absorption of model therapeutics inulin, hydrocortisone, and mesalamine two- to tenfold in ex vivo tissue, depending on location in the GI tract. In pigs, ultrasound induced transient cavitation with negligible heating, leading to an order of magnitude enhancement in the delivery of mesalamine, as well as successful systemic delivery of a macromolecule, insulin, with the expected hypoglycemic response. In a rodent model of chemically induced acute colitis, the addition of ultrasound to a daily mesalamine enema (compared to enema alone) resulted in superior clinical and histological scores of disease activity. In both animal models, ultrasound treatment was well tolerated and resulted in minimal tissue disruption, and in mice, there was no significant effect on histology, fecal score, or tissue inflammatory cytokine levels. The use of ultrasound to enhance GI drug delivery is safe in animals and could augment the efficacy of GI therapies and broaden the scope of agents that could be delivered locally and systemically through the GI tract for chronic conditions such as inflammatory bowel disease.

INTRODUCTION

Delivering drugs through the gastrointestinal (GI) tract is highly desirable because of its potential to be minimally invasive and enable superior kinetics of administration; yet, GI delivery is generally limited to small molecules (1). Even the delivery of small molecules can be challenging, with drugs often requiring specialized formulations to stabilize the compound and provide optimal absorption. Moreover, during certain pathophysiologic states such as diarrhea, small molecules may have limited opportunity for absorption due to rapid transit in the GI tract. Additionally, there are many macromolecular drugs that would benefit from GI delivery, including nucleic acids, peptides, and monoclonal antibodies. Therefore, a platform that enables the delivery of a broad range of therapeutics without the need for time-consuming and costly reformulation could present a paradigm shift in delivery science and have wide clinical impact. We hypothesized that a physical force, ultrasound, would be capable of enhancing the delivery of macromolecules across GI barriers while circumventing the need for extensive formulation development.

Ultrasound is a longitudinal pressure wave with frequencies above the audible range (>20 kHz). Clinically, ultrasound is applied in a variety of settings, including ultrasonography, tumor ablation, and lithotripsy (2, 3), which mainly use high frequencies (>1 MHz). At low frequencies (<100 kHz), ultrasound has unique properties including the ability to transiently permeabilize and propel therapeutic substances into tissue by a phenomenon known as transient cavitation (4). Transient cavitation can be induced using several ultrasound probe configurations, including axial and radial emission. Furthermore, the optimal ultrasound configuration can be adjusted depending on the condition being treated, maximizing the potential generalizability of this modality.

Using a physical delivery modality such as ultrasound to maximize drug delivery to the GI tract could have broad clinical utility. Patients with inflammatory bowel disease (IBD), for example, are faced with a dearth of effective treatment options. These patients have high

morbidity and compromised quality of life (5). First-line therapy for the most common IBD subtype, ulcerative colitis, includes aminosalicylates administered orally or rectally, with the latter being recognized as more efficacious, particularly in patients with mild to moderate disease activity (5, 6). However, rectal (enema) treatment efficacy is directly dependent on retention time and tissue absorption of the drug (6, 7), which is challenging for patients suffering from diarrhea with frequent bowel movements. Higher mucosal concentrations of these agents have been shown to correlate with decreased disease activity (6). Therefore, the use of ultrasound to maximize local mucosal concentrations of aminosalicylates in the rectum while reducing the necessary retention time of the enema could be one potential application of this technology with major clinical impact and benefit for patients who must currently self-administer medicated enemas.

In addition to therapeutic delivery to the rectum locally, a physical delivery modality could allow for the systemic delivery of a wide range of compounds, shifting the way in which diseases are targeted and treated. Here, we evaluated the delivery of model therapeutics with a broad range of molecular weights in the GI tract *ex vivo* and *in vivo* in both small and large animal models, thereby demonstrating adaptability to various clinical and research scenarios.

RESULTS

Ultrasound enhances drug delivery *ex vivo*

To understand whether ultrasound could safely permeabilize GI tissue and identify optimal conditions for ultrasound-mediated GI delivery (UMGID), we developed an *ex vivo* platform comprising fresh porcine GI tissue mounted in Franz diffusion cells (Fig. 1A). We focused on the use of low-frequency (<100 kHz) ultrasound, given previous data supporting increased cavitation activity at typical intensities compared to high-frequency (>1 MHz) ultrasound at the same intensities (8). First, we compared the transport of tritiated glucose as a model permeant across all major segments of the GI tract using 20-kHz ultrasound at an intensity of 7.5 W/cm². We found that the mass of glucose delivered to the GI tissue was enhanced by as much as an order of magnitude when delivery was combined with 1 min of ultrasound treatment (Fig. 1, B and C).

To identify the optimal parameters of UMGID, we tested glucose delivery using three distinct frequencies—20, 40, and 60 kHz—at three separate intensities for each frequency in the GI tract. Because transient cavitation was hypothesized to be the dominant mechanism, these frequencies were chosen to ensure that the cavitation threshold could be exceeded. To assess the effect of analyte molecular weight and because glucose is actively absorbed across the GI tract by glucose transporters, we carried out this study using inulin (5000 daltons), which is not actively absorbed by the GI epithelium (9). Transport of these molecules was enhanced at ultrasound frequencies of 20 and 40 kHz compared to 60 kHz (Fig. 1, C and D, and fig. S1). Delivery was relatively insensitive to the intensity at all frequencies.

Having shown that ultrasound enhances drug delivery in the GI tract, we focused on the delivery of topical therapeutics currently used for the management of IBD. Radiolabeled mesalamine (5-aminosalicylic acid) and hydrocortisone were administered with UMGID *ex*

vivo using 20- and 40-kHz axial emissions. Mesalamine was evaluated in the small and large intestine, and hydrocortisone was evaluated throughout the GI tract, in keeping with their respective clinical applications. All treatment times were 1 min, ensuring a treatment regimen that would be compatible with clinical endoscopy as well as patient self-administration. Mesalamine delivery to the intestine and colon was maximal at 20 kHz (Fig. 1E), with about threefold more drug delivered than control (no ultrasound). Hydrocortisone delivery was enhanced two- to fivefold throughout the GI tract using both 20- and 40-kHz ultrasound (Fig. 1E and fig. S1).

To characterize the tissue distribution of permeants delivered using ultrasound, we used fluorescently labeled dextran (3 and 70 kD). Without ultrasound, there was no visible permeation of either dextran into colonic tissue (Fig. 1F), whereas with 20-kHz ultrasound, both 3- and 70-kD dextran penetrated throughout the tissue ex vivo. This was also observed in the radiometric experiments, which showed significantly more permeant in the tissue than in the receiver chamber (fig. S2).

UMGID enhances drug delivery through transient cavitation

On the basis of previous studies of ultrasound transmission through liquids, we postulated that three mechanisms could be contributing to the observed enhancement in tissue drug delivery with ultrasound: (i) heating, (ii) acoustic streaming, and (iii) transient cavitation (8, 10, 11). To elucidate the dominant mechanism, we delivered tritiated glucose to the small intestine under the isolated effects of (i) heating the tissue, (ii) agitation to mimic streaming, and (iii) sonication with 1-MHz ultrasound below the cavitation threshold. These regimens were compared to delivery using 20- and 40-kHz ultrasound.

Ex vivo treatment of tissue mounted in Franz diffusion cells with 20-kHz ultrasound at 7.5 W/cm² raised the donor chamber temperature from 21.0° ± 1.2°C (*n* = 3) to 38.5° ± 1.0°C (*n* = 3) immediately after treatment ended. In a separate set of experiments, the temperature was monitored locally in pigs in vivo using a thermocouple in the rectum and was found to increase only 1.04° ± 0.66°C (*n* = 3) as a result of 20-kHz ultrasound treatment at the same intensity used in the diffusion cells. The negligible rise in temperature supports the hypothesis that thermal effects are not responsible for an increase in drug delivery with ultrasound. Indeed, ex vivo non-ultrasound heating of small intestine tissue to 40°C for 2 or 5 min provided no enhancement in glucose delivery compared to the 20-kHz ultrasound control (Fig. 2A). Similarly, acoustic streaming and agitation (sonication at 1 MHz, matching energy of 40-kHz ultrasound at 13.4 W/cm²) did not enhance glucose delivery (Fig. 2B). Although stirring enhanced delivery by about twofold compared to passive delivery, this was still significantly less glucose than that delivered with 40-kHz ultrasound (Fig. 2B). Thus, thermal effects and acoustic streaming do not appear to contribute significantly to enhancing drug delivery using UMGID.

To confirm that the mechanism of enhanced drug delivery through ultrasound is transient cavitation, we visualized pitting in aluminum foil samples (12) and took acoustic measurements in vivo in pigs. The number of pits generated with 20- and 40-kHz ultrasound was found to be significantly greater than the number generated with 60-kHz ultrasound (Fig. 2,C and D). Conversely, nopitting was visible when 1-MHz ultrasound was applied. We

then investigated the generation of transient cavitation in vivo in pigs. For a given driving frequency (f), cavitation generates acoustic emissions at subharmonics (f/n) and higher harmonics (nf) for integer values of n , with amplitudes that vary on the basis of the excitation intensity and frequency. Specifically, the $f/2$ subharmonic is commonly used as an indication of the onset of cavitation (13). From in situ acoustic data on three separate animals undergoing UMGID at 20 kHz, we observed the characteristic $f/2$ cavitation subharmonic and $2f$ harmonic in all measurements, confirming the generation of acoustic cavitation (Fig. 2E). As expected, these characteristic signatures were not present when the ultrasound was off (Fig. 2F). Although measurements were only taken for periods of 32 ms, cavitation phenomena occurred on the order of microseconds, making this sufficient for detection (13). Together, these data suggest that 20 or 40 kHz would provide optimal drug delivery results in vivo, enabling drug delivery across the GI tissue barrier by transient cavitation.

We calculated the theoretical pore sizes generated in porcine small intestine samples ex vivo using hindered transport theory as a result of treatment with 20-kHz ultrasound, with radiolabeled glucose and inulin as the model permeants (eqs. S1 to S4) (14). The permeability of glucose and inulin was significantly greater when delivered with ultrasound ($P = 0.008$, two-tailed Student's t test) (Fig. 2G, fig. S3, and table S1). Additionally, the upper limit of the calculated theoretical pore radii in untreated intestine was found to be 53 Å, compared to an upper limit of 90 Å in treated samples (Fig. 2G).

Axial UMGID significantly enhances drug delivery in swine

Given the efficacy of UMGID observed ex vivo, we hypothesized that this technology would enable greater enhancement in vivo (15). Two different configurations of UMGID were tested in vivo in small and large animals: axial emission in swine (Fig. 3A) and radial emission in mice. Both handheld devices were lightweight with dimensions amenable to insertion into the rectum. In vivo evaluation was first performed using axial emission of 20-kHz ultrasound in Yorkshire pigs. The size of the probe tip that was inserted was comparable to the size of a standard colonoscope. The tolerability of a single treatment and that of repeated administration over a 2-week period were investigated using rectal tissue biopsies. Biopsies of colon tissue from the pigs demonstrated only minor epithelial disruption in <5% of the treated area examined, as determined by a clinical pathologist (Fig. 3B and fig. S4A). There was minor cellular disarray in the control samples, which was determined to be an artifact due to the fixation procedure. In the samples treated with ultrasound, patchy saponification of the adipose tissue was noted. Further, minimal congestion of intramucosal capillary vessels located in the superficial submucosa was noted. There was no evidence of epithelial damage, and mucosal integrity was observed (Fig. 3B). Repeated daily administration over a 2-week period was clinically well tolerated, and histological examination of the rectum and abdominal organs showed normal architecture of all abdominal organs (fig. S4). The rectal epithelium, for example, showed intact mucosal wall, and the epithelium had normal structure with the presence of crypts. All other internal organs showed normal pathology with no signs of ultrasound-induced injury.

The efficacy of mesalamine delivery was then assessed in vivo. A mesalamine enema at the concentration and volume used clinically [Rowasa (mesalamine), 4 g in 60-ml suspension (16)] was instilled in the swine rectum, immediately followed by a single application of 20kHz ultrasound at 7.5 W/cm² for 1 min. Tissue biopsies taken immediately after UMGID showed a significant ~22-fold increase in tissue uptake of the drug using ultrasound compared to colonic tissue exposed to the drug without ultrasound (Fig. 3C). One-half of the non-ultrasound samples had a drug content below the limit of gas chromatography–mass spectrometry detection (50 ng/g tissue). ¹H Nuclear magnetic resonance (NMR) spectroscopy confirmed the chemical stability of mesalamine after treatment with ultrasound (fig. S5).

The delivery of insulin, a model biologic, was also evaluated to determine the potential of UMGID to deliver larger, biologically active molecules. The same 1-min ultrasound treatment with an insulin enema resulted in a robust hypoglycemic response (Fig. 3D). Forty minutes after UMGID, control animals experienced no drop in blood glucose (109 ± 9% of initial levels), whereas ultrasound-treated animals were at a significantly lower level on average (83 ± 9%) ($P = 0.02$, two-tailed Student's *t* test), indicating the ability of ultrasound to drive insulin across the colon tissue barrier. Sonication of insulin was similarly found to have no impact on its active protein structure (fig. S6). Successful delivery of drugs varying in molecular weight by an order of magnitude supports the likely broad applicability of UMGID.

Radial UMGID is safe and resolves acute colitis activity in mice

The clinical relevance of the enhancement in mesalamine delivery was analyzed in a murine model of dextran sodium sulfate (DSS)–induced acute colitis. This murine model was chosen because it is recognized to not benefit from topical mesalamine administration (17). Therefore, improvement in disease indices in this model as a result of ultrasound treatment would underscore the impact of UMGID. Radial UMGID was used given the colonic anatomy and the often circumferential nature of colitis involvement.

The tolerability of daily probe insertion and probe insertion followed by sonication was first tested in healthy animals in the absence of colitis. Ultrasound was administered daily (Fig. 4A) using a custom-designed ultrasound probe with dimensions amenable to insertion directly into the mouse colon (probe diameter, 3 mm) (Fig. 4B). Histological examination at day 14 was selected to assess the effect of repeated dosing and to allow for comparison to results from animals with induced disease receiving a clinically utilized 14-day course of treatment. Treatment was well tolerated, and all animals were free of clinical signs of distress over the 14-day period. Additionally, there was no statistical difference in the animals' hematocrit or hemoglobin as a result of ultrasound treatment compared to controls, suggesting that the device does not induce gross bleeding (Fig. 4C).

After the 14-day course of treatment, colonic tissue was scored histologically for degree of inflammation and architectural distortion (Fig. 4D). The scores for these animals were comparable to those of untreated (control) animals and were significantly lower than the scores of animals with induced disease, suggesting that ultrasound treatment in healthy animals is well tolerated. In addition, surrounding organs in the body cavity were examined

to assess the potential of longer-range adverse effects. On gross examination, the liver, spleen, pancreas, kidney, and small intestine appeared normal without any ecchymoses noted on the organs after treatment (fig. S4B). Additionally, blinded evaluation of these organs histologically by a clinical pathologist determined the tissue to be of normal architecture with no histological abnormalities in both the control and sonication groups. Clinically, these animals were free from diarrhea and occult bleeding (total fecal score, Fig. 4E). Finally, no statistical difference was found in the expression levels of the proinflammatory cytokines including tumor necrosis factor- α (TNF- α), interferon- γ (IFN- γ), interleukin-6 (IL-6), or IL-17 between treatment groups ($P > 0.05$, one-way ANOVA with multiple comparisons) (Fig. 4F). Together, these data in mice support the safety of this drug delivery modality in the GI tract.

Colitis was induced in mice with DSS given ad libitum for 7 days with concurrent mesalamine enema/ultrasound treatment starting on day 2 (Fig. 5A). The administration of mesalamine in combination with ultrasound given daily (QD) as well as every other day (QOD) enabled significantly faster recovery from clinical signs of colitis compared to daily administration of mesalamine enema alone (the current standard of care), as assessed by the total fecal score (Fig. 5B). For both ultrasound treatment groups, total fecal scores were 4 on day 14, although QD ultrasound worked more quickly and reduced colitis faster than QOD.

In addition to the total fecal score, colonic tissue histology was evaluated at the end of the trial in a blinded fashion (Fig. 5, C and D). The ultrasound treatment QD group had a statistically lower histology score than any other group with induced disease, in agreement with the improved fecal scores. The tissue in the ultrasound treatment QD group appeared to have less erosion of the epithelium and only minor shortening of the crypts when compared to the other colitis groups (Fig. 4C).

DISCUSSION

Here, we present the preclinical use of ultrasound as an active drug delivery modality throughout the GI tract. We found that ultrasound was able to enhance the delivery of model drug compounds with a wide range of molecular weights in all parts of the GI tract *ex vivo*; more surprising was the relatively short treatment time required for this: 1 min of total ultrasound exposure. We tested two configurations *in vivo*: axial emission in pigs and radial emission in mice. Ultrasound in combination with a medicated enema was found to significantly improve disease indices and also have the capacity for macromolecule delivery: mesalamine delivered to rodents reduced the severity and duration of colitis compared with the standard of care (free drug enema), and insulin delivered to pigs reduced blood glucose. The trend toward improved clinical outcome in rodents treated every other day suggests that such a regimen may be useful in less severe cases of colitis and in patients with suboptimal adherence to medication, a significant issue in the clinic today (18). A mechanistic investigation confirmed the generation of cavitation *in vivo*, and further tests showed thermal effects and acoustic streaming to play a minimal role in enhancing drug delivery. The superior disease outcomes, both clinically and histologically, of daily ultrasound treatment compared to the current standard of care are exciting and suggest that UMGID could enable

remission to be achieved with shorter treatment regimens. Moreover, it provides a solution for accelerated drug delivery in clinical settings where rapid disease-associated GI transit time limits the absorption of therapeutics (19). As a result, our technology may eliminate the need for extended enema retention.

Axial emission in swine was demonstrated to be safe on the basis of histological examination of the tissue and clinical monitoring of the animal. Although tissue biopsies taken immediately after treatment showed minor disruption to the tissue, these findings were not present in tissue biopsies taken after repeated treatment, suggesting that the tissue can recover fully from the treatment, highlighting its tolerability. The order of magnitude enhancement observed in mesalamine delivery is indicative of the potential power of UMGID. Further, the delivery of insulin as a model biologic highlights the ability of axial emission to achieve systemic delivery of larger molecules through the rectum and potentially through the varying segments of the GI tract while retaining their function. Local delivery of biologics has the potential to be useful in a variety of diseases. For ulcerative colitis, for example, the local delivery of monoclonal antibodies targeting TNF could be beneficial to down-regulate proinflammatory processes (20). This technology in its present form could also be beneficial in the local delivery of chemotherapeutics and biologics in the rectum for the treatment of colorectal cancer (21). Indeed, current strategies to achieve local delivery of these agents largely rely on formulation techniques, which suffer from low loading efficiencies and lack broad applicability to deliver many drugs (22, 23).

In addition to axial emission, radial emission was tested in a clinically relevant murine colitis model. The most efficacious treatment of mild to moderate colitis is rectal administration (5, 24). However, active disease can make retention of the medication difficult. For example, the current procedure for the rectal administration of mesalamine for the treatment of IBD requires patients to first empty their bowels. They are then instructed to lie on their left side. The patient must insert an applicator tip into the rectum and gently infuse the drug. Patients are instructed to remain in this position for at least 30 min and to retain the enema overnight (25). This creates a precarious and uncomfortable experience that must be endured nightly. This is particularly challenging for patients with active colitis who are experiencing urgency with frequent bowel movements. Even when this regimen is strictly adhered to, disease relapse rates are high (26). To test whether UMGID has the capacity to promote rapid delivery of mesalamine and thereby enhance treatment efficacy, an ultrasound probe with radial emission was used for its ability to permeabilize a larger area of tissue. The use of a custom-designed ultrasound probe with a shaft diameter of 3 mm is indicative of the ability to significantly miniaturize this technology. With additional study, we believe this could be miniaturized further to enable other form factors, such as ingestible capsules. Translating UMGID into the clinic for the treatment of IBD will involve further optimization of the radially emitting probes to maximize radial acoustic emission in the human rectum. This development will require large animal model testing under good laboratory practices ensuring safety and efficacy to inform an Investigational Device Exemption application to the U.S. Food and Drug Administration.

UMGID has many potential applications ranging from localized site-specific treatment with anti-inflammatories to the broader delivery of macromolecules. The current format of

administration limits application of the technology somewhat to diseases requiring delivery through the rectum. However, the ability to generate ultrasound in multiple configurations in small, portable form factors amenable to at-home self-administration supports the generalizability of UMGID and its tunability. Such ease of use is paramount for broad clinical and research applicability. In the immediate-use case of rectal delivery for diseases such as IBD where enemas are already established as the standard of care, patients may use a small, handheld device that emits ultrasound radially to achieve a high degree of circumferential tissue permeability, increasing drug delivery. Continued improvement in ultrasound miniaturization could allow for a variety of different operating formats to enable convenient ultrasound exposure to all parts of the GI tract, including ingestible ultrasound-emitting capsules to facilitate systemic delivery in a convenient manner (27).

Our technology could be miniaturized to dimensions compatible with ingestion, allowing for ingestible ultrasound-emitting capsules for systemic delivery. On the basis of the studies described here, ultrasound technology has the potential to deliver substances such as nanoparticles, monoclonal antibodies, or vaccines to modulate mucosal immune responses (28, 29). Additionally, ultrasound could potentially enable the delivery of new classes of therapeutics such as DNA- and RNA-based therapeutics, where delivery requires overcoming several biological barriers (30). With further study, this technology could prove invaluable in both clinical and research settings, enabling improved therapies and expansion of research techniques applied to the GI tract as well as new medical devices to enable local rectal delivery and, eventually, oral administration using ingestible electronic devices.

MATERIALS AND METHODS

Study design

The purpose of this study was to investigate the safety, tolerability, and utility of ultrasound-mediated drug delivery in the GI tract in tissue *ex vivo* as well as *in vivo* in Yorkshire pigs and mice. Low-frequency (<100 kHz) ultrasound was used and administered directly to GI tissue. This treatment was compared to controls consisting of untreated tissue. The treatment time used was 1 min. Fresh, porcine GI tissue was mounted in Franz diffusion cells and randomly selected to receive either ultrasound treatment or no treatment. *Ex vivo* delivery efficacy was assessed by quantifying the delivery of radiolabeled permeants into and through tissue.

Rectal delivery in pigs and mice was tested using 20- and 40-kHz ultrasound compared to delivery without ultrasound. The 20-kHz ultrasound was chosen because it maximizes cavitation activity and is above the human range of hearing. In mice, 40 kHz was used because of technical limitations preventing a device amenable to rectal administration in rodents having a lower frequency. Animals were randomly assigned to receive a particular treatment, consisting of a combination of mesalamine enema and ultrasound administration. In pigs, delivery of mesalamine was quantified from collected tissue biopsies, and delivery of insulin was measured by blood glucose response over 40 min. For mice with DSS-induced acute colitis, the effect of rectal ultrasound was determined by blood markers, fecal score, and cytokine levels. For both pigs and mice, histological evaluation was performed in a blinded fashion by a clinical pathologist to assess the safety of ultrasound treatment.

The sample sizes, determined before study initiation, were based on published reports of mesalamine quantification from biopsies in humans as well as our preliminary ex vivo data (6). Power calculations were carried out on the basis of the enhancement in delivery observed in the pig studies using ultrasound as well as previously published reports examining fecal scores (7). Nosamples were excluded from analysis in this study.

Tissue preparation

The Massachusetts Institute of Technology Committee on Animal Care approved all animal-related research aspects of this study. GI tissue from Yorkshire pigs was procured within 20 min of sacrifice, stored at 4°C, and used within 6 hours of euthanization. The tissues were obtained from Research 87 Inc. The tissues were washed with phosphate-buffered saline (PBS), and excess fat was dissected away. With the exception of the tongue, all tissues were used as received. The tissues were then sectioned and mounted in Franz diffusion cells (15 mm diameter, PermeGear) with the luminal side facing the donor chamber (Fig. 1A). Because of significant variability in tongue tissue thickness, the top surface was isolated with an electric dermatome (Zimmer Orthopedic Surgical Products) to a thickness of 700 µm and mounted. After all tissues had been dissected and mounted in Franz diffusion cells, the cells were randomly assigned to the various experimental groups.

Ultrasound treatment

Ultrasound intensities were calibrated by calorimetry using an unlined dewar. Calorimetry was used because this specific method is commonly used in the literature to estimate ultrasonic power (31). The three powers at 20 kHz were 2.5, 5, and 7.5 W/cm². At 40 kHz, they were 7.3, 10.5, and 13.4 W/cm². At 60 kHz, the powers were 9.6, 11.5, and 12.4 W/cm². The difference in powers tested at each frequency was due to the sensitivities and efficiency of each ultrasound generator. Regardless of frequency or power, all treatments lasted for a total of 1 min of ultrasound exposure using a 50% duty cycle (5 s on and 5 s off) with the ultrasound horn tip 3 mm away from the surface of the tissue.

Immediately before ultrasound treatment, a solution (1 mg/ml) containing radiolabeled material was added to the donor chamber. Ultrasonic frequencies of 20, 40, and 60 kHz were generated using three separate ultrasound generators (Sonics and Materials Inc.), the VCX 500, VCX 130, and a custom order probe, respectively. The probes provide axial emission of ultrasound. Each probe has a 13-mm diameter tip. The three separate powers at each frequency were tested. Treatment lasted for 1 min of ultrasound exposure using a 50% duty cycle. Permeant delivery was then quantified as described in Supplementary Methods.

Mixing, temperature, and high-frequency ultrasound studies

Tissue samples were mounted in Franz diffusion cells and exposed to stirring, increased temperature, or 1-MHz ultrasound to determine the role in glucose uptake, as described in Supplementary Methods.

Effect of sonication on therapeutic compound structure

The impact of sonication with 20-kHz ultrasound on chemical structure was investigated using mesalamine, hydrocortisone, and insulin, as detailed in Supplementary Methods.

Porcine model

Both female and male Yorkshire pigs between 45 and 80 kg in weight were used for this study on the basis of the availability of sex from the vendor. Before every experiment, the animal was fasted overnight. The animals were sedated, and the rectum was cleared with a tap water enema, as detailed in Supplementary Methods. The drug of interest (mesalamine or insulin) was then instilled in the rectum, ultrasound was administered, and drug delivery was quantified (see Supplementary Methods).

In vivo cavitation detection

Rectal UMGID at 20 kHz was performed on three sedated animals, and an omnidirectional hydrophone (Teledyne Reson TC4013, 1 Hz to 170 kHz sensitivity range) was coupled to the lower anterior abdominal skin with ultrasound gel. The hydrophone output was collected over a 32-ms interval at a sampling rate of 250 kHz on an oscilloscope (Rigol DS1204B), and data were postprocessed in MATLAB R2014a (MathWorks). Control (ultrasound off) traces were similarly collected from three sedated animals following the above methods. Data were processed as follows: an FFT was taken on each time series signal, a Gaussian filter was applied to reduce noise, and then all FFTs were averaged. Because of the sampling rate of 250 kHz on the oscilloscope, the FFT is limited to detecting acoustic signatures over the range of ultrasonic frequencies 0 to 125 kHz. This, however, is sufficient, given the fact that acoustic detection at $f/2$ is commonly used to determine the generation of cavitation particularly in medical applications and would be captured in this range for $f = 20$ kHz (13).

Insulin delivery in pigs

In addition to sedation (Supplementary Methods), a central venous catheter was placed in the femoral vein using the Seldinger technique to allow for frequent blood sampling. Blood samples were drawn to assess the animal's baseline blood glucose level, and then insulin and ultrasound were administered as described further in Supplementary Methods.

Chemically induced murine colitis model and treatment

Fifteen-week-old female C57BL/6 mice were purchased from Charles River Laboratories for the induction and treatment of DSS-induced colitis. Five animals were used per group. Acute colitis was then induced by administering DSS in the drinking water, and treatment was administered as described in Supplementary Methods. Acute colitis severity was determined through histological evaluation of the colon. Fecal consistency and the presence of blood were scored on the basis of published protocols with slight modifications as detailed in Supplementary Methods (7, 32).

UMGID treatment was administered to DSS mice starting on day 2. Treatment consisted of either a mesalamine enema alone or in combination with ultrasound. The enema consisted of mesalamine (66.6 mg/ml) in a 0.5% w/w carboxymethyl cellulose (Sigma-Aldrich) solution in PBS. Here, a custom-designed 40-kHz probe was fabricated to allow for insertion into the colon (Sonics and Materials Inc.). The shaft was 2 mm in diameter and contained two protrusions 3 mm in diameter at half-wavelength intervals to achieve radial ultrasound emission. The power of ultrasound treatment was calibrated to 4.0 W by calorimetry. The probe was inserted into the rectum and turned on for 0.5 s. The animals were monitored

daily for weight, fecal consistency, and the presence of fecal occult blood using Hemoccult cards (Beckman Coulter).

Safety and tolerability of the ultrasound probe

A separate cohort of animals with no induced disease was used to test the safety and tolerability of ultrasound in the rectum, as described in Supplementary Methods.

Statistical analysis

Statistical analysis for the ex vivo and in vivo porcine work was performed using two-tailed Student's *t* tests to determine statistical significance. Statistical analysis for the in vivo mouse work was performed using one-way ANOVA tests with multiple comparisons. Confidence intervals for regression slopes were constructed using normal-based 95% confidence intervals. Statistical significance was defined throughout as $P < 0.05$. All calculations were performed in MATLAB R2014a (MathWorks).

Supplementary Material

Refer to Web version on PubMed Central for supplementary material.

Acknowledgments

We thank Pentax for providing the endoscopic equipment used for this research and, in particular, M. Fina for facilitating access to the equipment. We thank M. Siddalls, C. Gallo, M. Patterson, R. Marini, J. Haupt, M. Jamiel, and C. Cleveland for help with the in vivo porcine work; J. Wardrobe for assistance with endoscopy consumables; A. Scherer-Hoock for help with the in vivo mouse work; the Hope Babette Tang (1983) Histology Core Facility; J. Wyckoff of the microscopy core facility in the Swanson Biotechnology Center for imaging colon samples. We thank H. Kuhn for assistance with RNA extraction. We are grateful to all members of the Blankschtein and Langer laboratories, especially B. C. Tang and Y.-A. L. Lee, and to O. Veiseh for helpful methodological suggestions. We also thank members of the Massachusetts General Hospital GI Unit for helpful discussions.

Funding: This work was funded by the NIH (grant nos. EB-00351, EB-000244, and CA014051) and the Max Planck Research Award, Award Ltr Dtd. 2/11/08, Alexander von Humboldt-Stiftung Foundation (to R.L.). G.T. was supported in part by NIH grant T32-DK007191-38-S1.

REFERENCES AND NOTES

1. Ensign LM, Cone R, Hanes J. Oral drug delivery with polymeric nanoparticles: The gastrointestinal mucus barriers. *Adv Drug Deliv Rev.* 2012; 64:557–570. [PubMed: 22212900]
2. Pavlin CJ, Harasiewicz K, Sherar MD, Foster FS. Clinical use of ultrasound biomicroscopy. *Ophthalmology.* 1991; 98:287–295. [PubMed: 2023747]
3. Kennedy JE. High-intensity focused ultrasound in the treatment of solid tumours. *Nat Rev Cancer.* 2005; 5:321–327. [PubMed: 15776004]
4. Holland CK, Apfel RE. Thresholds for transient cavitation produced by pulsed ultrasound in a controlled nuclei environment. *J Acoust Soc Am.* 1990; 88:2059–2069. [PubMed: 2269722]
5. Seibold F, Fournier N, Beglinger C, Mottet C, Pittet V, Rogler G. Swiss IBD cohort study group, Topical therapy is underused in patients with ulcerative colitis. *J Crohns Colitis.* 2014; 8:56–63. [PubMed: 23566922]
6. Frieri G, Giacomelli R, Pimpo M, Palumbo G, Passacantando A, Pantaleoni G, Caprilli R. Mucosal 5-aminosalicylic acid concentration inversely correlates with severity of colonic inflammation in patients with ulcerative colitis. *Gut.* 2000; 47:410–414. [PubMed: 10940280]

7. Nakashima T, Maeda T, Nagamoto H, Kumakura T, Takai M, Mori T. Rebamipide enema is effective for treatment of experimental dextran sulfate sodium induced colitis in rats. *Dig Dis Sci*. 2005; 50(Suppl 1):S124–S131. [PubMed: 16184415]
8. Leighton, TG. *The Acoustic Bubble*. Academic Press; San Diego: 1997.
9. Veereman G. Pediatric applications of inulin and oligofructose. *J Nutr*. 2007; 137:2585S–2589S. [PubMed: 17951508]
10. Brotchie A, Grieser F, Ashokkumar M. Characterization of acoustic cavitation bubbles in different sound fields. *J Phys Chem B*. 2010; 114:11010–11016. [PubMed: 20698516]
11. Pelekasis NA, Gaki A, Doinikov A, Tsamopoulos JA. Secondary Bjerknes forces between two bubbles and the phenomenon of acoustic streamers. *J Fluid Mech*. 2004; 500:313–347.
12. Prentice P, Cuschieri A, Dholakia K, Prausnitz M, Campbell P. Membrane disruption by optically controlled microbubble cavitation. *Nat Phys*. 2005; 1:107–110.
13. Johnston K, Tapia-Siles C, Gerold B, Postema M, Cochran S, Cuschieri A, Prentice P. Periodic shock-emission from acoustically driven cavitation clouds: A source of the sub-harmonic signal. *Ultrasonics*. 2014; 54:2151–2158. [PubMed: 25015000]
14. Peck KD, Ghanem AH, Higuchi WI. Hindered diffusion of polar molecules through and effective pore radii estimates of intact and ethanol treated human epidermal membrane. *Pharm Res*. 1994; 11:1306–1314. [PubMed: 7816761]
15. Barr WH, Riegelman S. Intestinal drug absorption and metabolism I: Comparison of methods and models to study physiological factors of in vitro and in vivo intestinal absorption. *J Pharm Sci*. 1970; 59:154–163. [PubMed: 5411337]
16. Marshall JK, Irvine EJ. Putting rectal 5-aminosalicylic acid in its place: The role in distal ulcerative colitis. *Am J Gastroenterol*. 2000; 95:1628–1636. [PubMed: 10925961]
17. Vong LB, Tomita T, Yoshitomi T, Matsui H, Nagasaki Y. An orally administered redox nanoparticle that accumulates in the colonic mucosa and reduces colitis in mice. *Gastroenterology*. 2012; 143:1027–1036.e3. [PubMed: 22771506]
18. Robinson A. Review article: Improving adherence to medication in patients with inflammatory bowel disease. *Aliment Pharmacol Ther*. 2008; 27(Suppl 1):9–14. [PubMed: 18307644]
19. Brunner M, Ziegler S, Di Stefano AFD, Dehghanyar P, Kletter K, Tschurlovits M, Villa R, Bozzella R, Celasco G, Moro L, Rusca A, Dudczak R, Müller M. Gastrointestinal transit, release and plasma pharmacokinetics of a new oral budesonide formulation. *Br J Clin Pharmacol*. 2006; 61:31–38. [PubMed: 16390349]
20. Neurath MF. New targets for mucosal healing and therapy in inflammatory bowel diseases. *Mucosal Immunol*. 2014; 7:6–19. [PubMed: 24084775]
21. Karaca-Mandic P, McCullough JS, Siddiqui MA, Van Houten H, Shah ND. Impact of new drugs and biologics on colorectal cancer treatment and costs. *J Oncol Pract*. 2011; 7(Suppl 3):e30s–e37s. [PubMed: 21886509]
22. Capurso NA, Fahmy TM. Development of a pH-responsive particulate drug delivery vehicle for localized biologic therapy in inflammatory bowel disease. *Yale J Biol Med*. 2011; 84:285–288. [PubMed: 21966047]
23. Škalko-Basnet N. Biologics: The role of delivery systems in improved therapy. *Biologics*. 2014; 8:107–114. [PubMed: 24672225]
24. Danese S, Fiocchi C. Ulcerative colitis. *N Engl J Med*. 2011; 365:1713–1725. [PubMed: 22047562]
25. Wolf JM, Lashner BA. Inflammatory bowel disease: Sorting out the treatment options. *Cleve Clin J Med*. 2002; 69:621–626. [PubMed: 12184470]
26. Kedia P, Cohen RD. Once-daily MMX mesalamine for the treatment of mild-to-moderate ulcerative colitis. *Ther Clin Risk Manag*. 2007; 3:919–927. [PubMed: 18473016]
27. Bawiec CR, Sunny Y, Nguyen AT, Samuels JA, Weingarten MS, Zubkov LA, Lewin PA. Finite element static displacement optimization of 20–100 kHz flexural transducers for fully portable ultrasound applicator. *Ultrasonics*. 2013; 53:511–517. [PubMed: 23040829]
28. Cerutti A. Location, location, location: B-cell differentiation in the gut lamina propria. *Mucosal Immunol*. 2008; 1:8–10. [PubMed: 19079155]

29. Zhu Q, Talton J, Zhang G, Cunningham T, Wang Z, Waters RC, Kirk J, Eppler B, Klinman DM, Sui Y, Gagnon S, Belyakov IM, Mumper RJ, Berzofsky JA. Large intestine-targeted, nanoparticle-releasing oral vaccine to control genitorectal viral infection. *Nat Med*. 2012; 18:1291–1296. [PubMed: 22797811]
30. Morrow MP, Weiner DB. DNA drugs come of age. *Sci Am*. 2010; 303:48–53. [PubMed: 20583666]
31. Liu J, Lewis TN, Prausnitz MR. Non-invasive assessment and control of ultrasound-mediated membrane permeabilization. *Pharm Res*. 1998; 15:918–924. [PubMed: 9647359]
32. Cooper HS, Murthy SN, Shah RS, Sedergran DJ. Clinicopathologic study of dextran sulfate sodium experimental murine colitis. *Lab Invest*. 1993; 69:238–249. [PubMed: 8350599]
33. Li T, Chen H, Khokhlova T, Wang YN, Kreider W, He X, Hwang JH. Passive cavitation detection during pulsed HIFU exposures of ex vivo tissues and in vivo mouse pancreatic tumors. *Ultrasound Med Biol*. 2014; 40:1523–1534. [PubMed: 24613635]
34. Wirtz S, Neufert C, Weigmann B, Neurath MF. Chemically induced mouse models of intestinal inflammation. *Nat Protoc*. 2007; 2:541–546. [PubMed: 17406617]
35. Malkov VA, Serikawa KA, Balantac N, Watters J, Geiss G, Mashadi-Hosseini A, Fare T. Multiplexed measurements of gene signatures in different analytes using the Nanostring nCounter™ Assay System. *BMC Res Notes*. 2009; 2:80. [PubMed: 19426535]
36. Dechadilok P, Deen WM. Hindrance factors for diffusion and convection in pores. *Ind Eng Chem Res*. 2006; 45:6953–6959.
37. Stein, WD. Channels, Carriers, and Pumps: An Introduction to Membrane Transport. Elsevier Science; Amsterdam: 2012.
38. Tezel A, Sens A, Mitragotri S. Description of transdermal transport of hydrophilic solutes during low-frequency sonophoresis based on a modified porous pathway model. *J Pharm Sci*. 2003; 92:381–393. [PubMed: 12532387]
39. Horowitz SB, Moore LC. The nuclear permeability, intracellular distribution, and diffusion of inulin in the amphibian oocyte. *J Cell Biol*. 1974; 60:405–415. [PubMed: 4544299]
40. Schultz SG, Solomon AK. Determination of the effective hydrodynamic radii of small molecules by viscometry. *J Gen Physiol*. 1961; 44:1189–1199. [PubMed: 13748878]

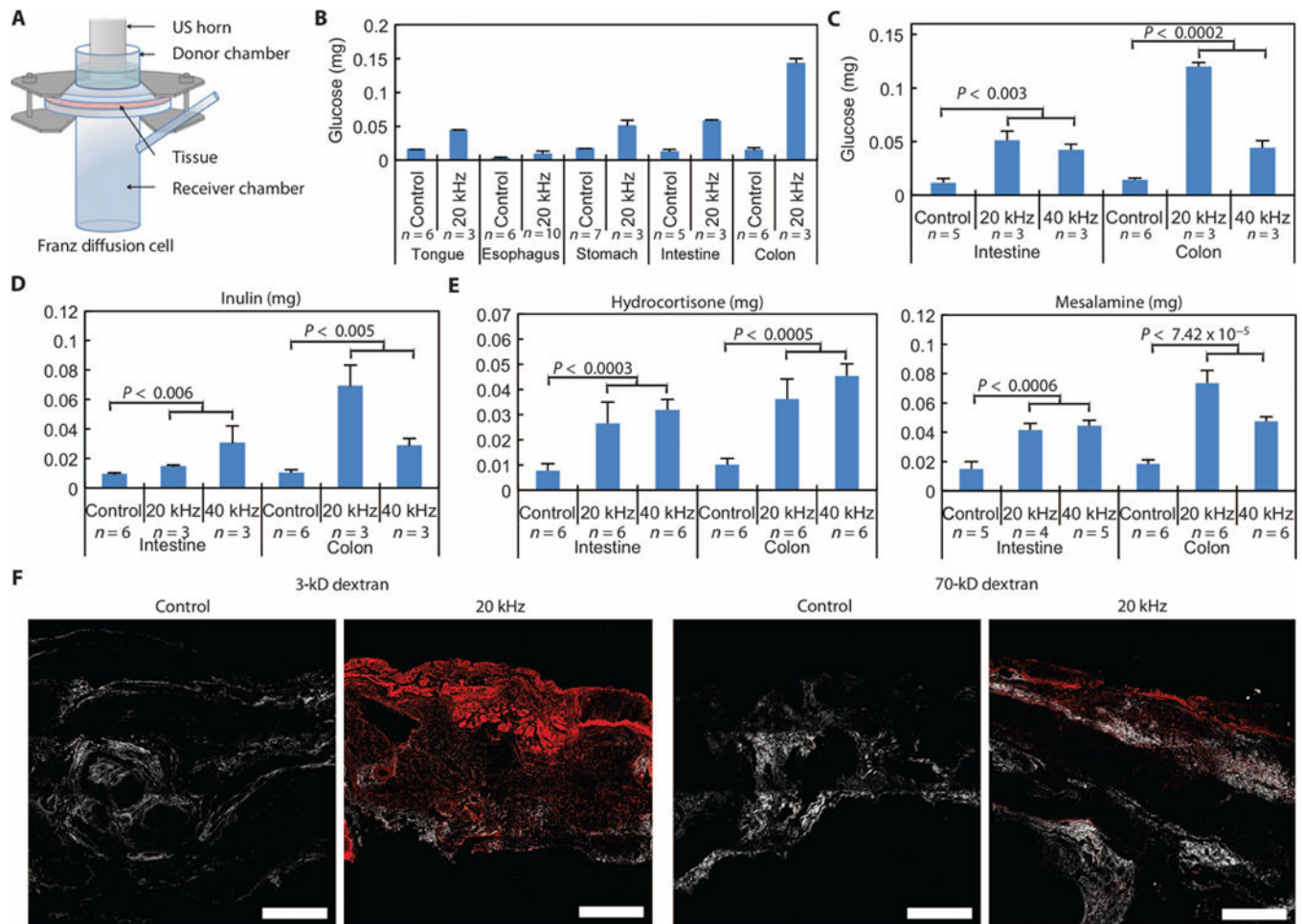


Fig. 1. Ex vivo characterization of UMIGD

(A) Ex vivo experimental setup, the Franz diffusion cell. A section of fresh GI tissue is shown positioned between a donor and receiver chamber. US, ultrasound. (B) Comparison of the amount of glucose delivered to various tissues of the GI tract with 20-kHz ultrasound at 7.5 W/cm² and without ultrasound (control) for 2 min with the horn set to pulse (50% duty cycle of 5-s on and 5-s off, resulting in 1 min of ultrasound exposure). (C to E) Survey of glucose (C), inulin (5 kD) (D), hydrocortisone (E), and mesalamine (E) delivery—all at 1 mg/ml—to porcine intestine and colon ex vivo using 20- and 40-kHz ultrasound at the lowest intensity considered for each frequency. Treatment duration was 1 min of ultrasound at a 50% duty cycle, as described in (B). (F) Multiphoton microscopy of cross sections of colonic tissue exposed to dextrans labeled with Texas red with and without 20-kHz ultrasound. The red channel and second harmonic (to show structural elements of the tissue) are shown. Scale bars, 500 μ m. Data in (B) to (E) are averages \pm 1 SD. Sample sizes indicated are biological replicates. Each experiment was performed once. Because not all experiments could be performed from one organ, controls were run for each additional organ procured to account for potential intertissue variability. *P* values in (C) to (E) were determined by two-tailed Student's *t* tests.

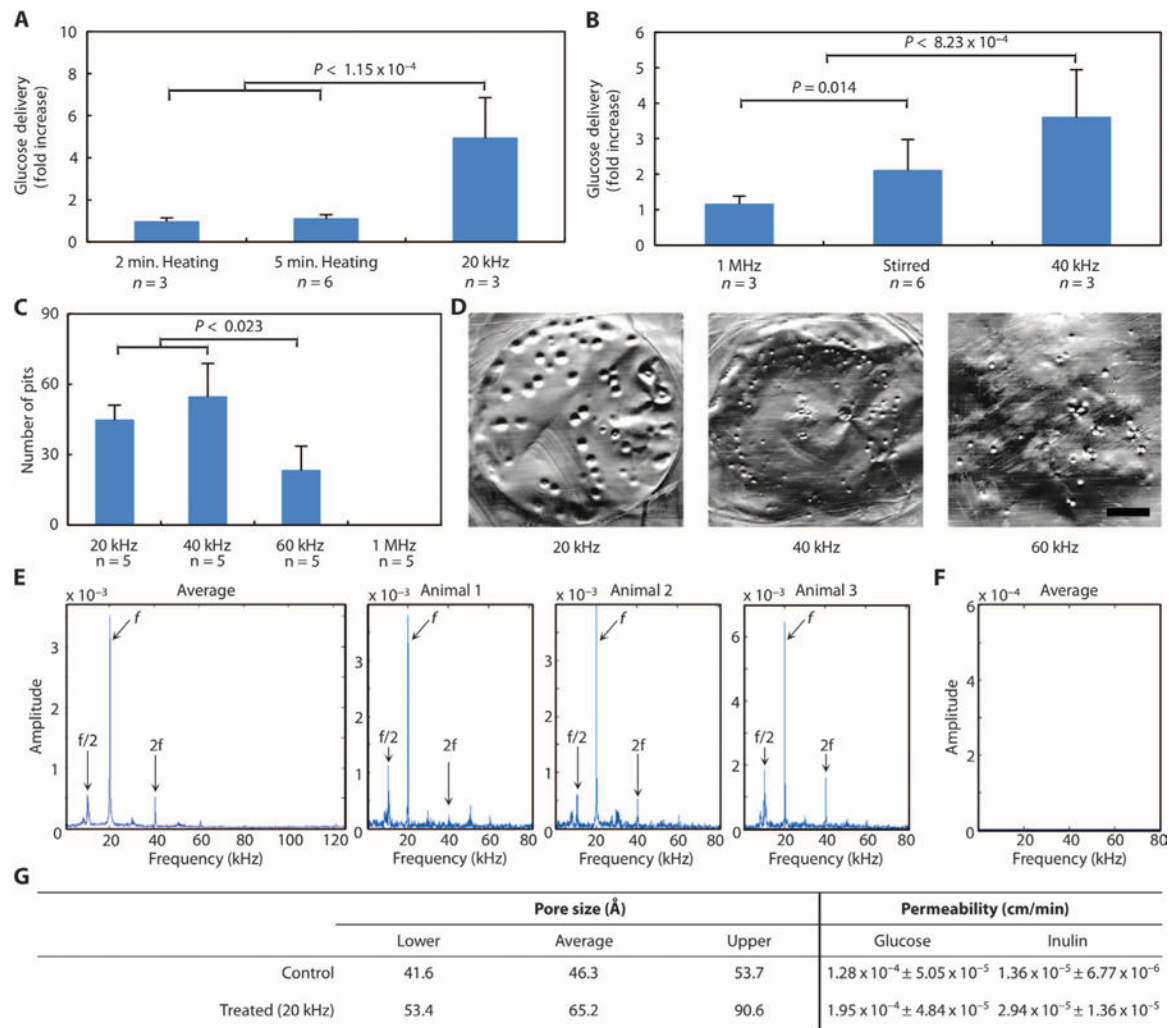


Fig. 2. Ex vivo and in vivo investigation of the mechanism of drug delivery enhancement with ultrasound

(A) Relative enhancement in glucose delivery to small intestine as a result of 40°C heating for 2 or 5 min or 20-kHz ultrasound at 7.5 W/cm² at a duty cycle of 50% for 2 min total. (B) Relative enhancement in glucose delivery to small intestine as a result of treatment with 1-MHz ultrasound set to 2 W/cm² (5.22 W actual) for 3.4 min, stirring of the donor chamber, or 40-kHz ultrasound set to an intensity of 13.4 W/cm². (C) Number of pits generated in aluminum foil after treatment with 20-, 40-, 60-kHz, or 1-MHz ultrasound for 2 s at the highest intensity considered for each frequency. In (A) to (C), data are averages \pm 1 SD; *P* values were determined by one-way analysis of variance (ANOVA) with multiple comparisons. (D) Representative images of pitted aluminum foil samples treated with either 20-, 40-, or 60-kHz ultrasound. Scale bar, 3 mm. (E and F) Averaged Gaussian filtered amplitude spectrum of six fast Fourier transforms (FFTs) taken on in situ acoustic data collected externally in vivo in pigs during *f* = 20 kHz UMGID along with a representative amplitude spectrum for each repeat (E) and a control when ultrasound was not on (F). (G) Estimation of pore size radii created in porcine small intestine tissue and permeability

(averages \pm 1 SD) of glucose and inulin as a result of ultrasound exposure using the aqueous porous pathway model.

Author Manuscript

Author Manuscript

Author Manuscript

Author Manuscript

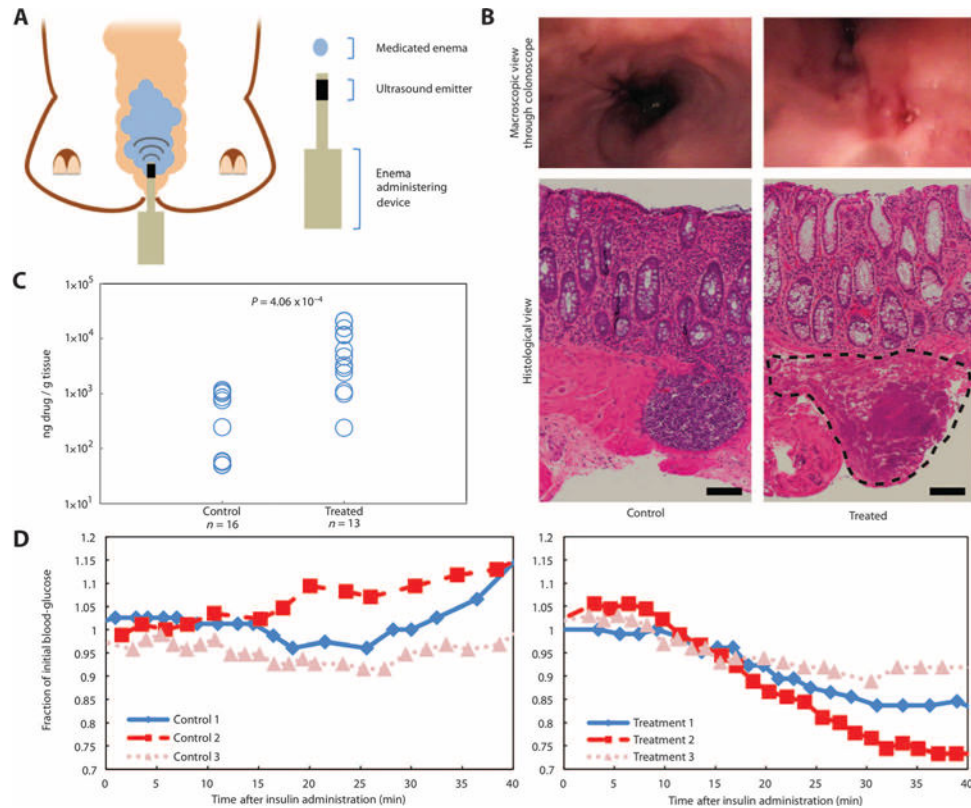


Fig. 3. In vivo axial UMGID in pigs

(A) Experimental setup showing placement of a medicated enema and insertion of the 20-kHz ultrasound probe in the rectum of a pig. (B) Representative macroscopic (top) and histological (bottom) views of the rectum not treated with ultrasound (control) or a single administration of 20-kHz ultrasound. The outlined area indicates minor localized saponification of the muscularis in <5% of the treated area examined. Scale bars, 100 μ m. (C) Mesalamine drug content in colon tissue biopsies normalized by the mass of the tissue biopsy without (control) and with (treated) a single administration of 20-kHz ultrasound. Each point represents one biological replicate. P value determined by two-tailed Student's *t* test. (D) Animals' blood glucose normalized to its initial value as a result of the placement of an enema containing 100 U of insulin without (left) or with (right) a single administration of 20-kHz ultrasound. Each individual curve is a biological repeat.

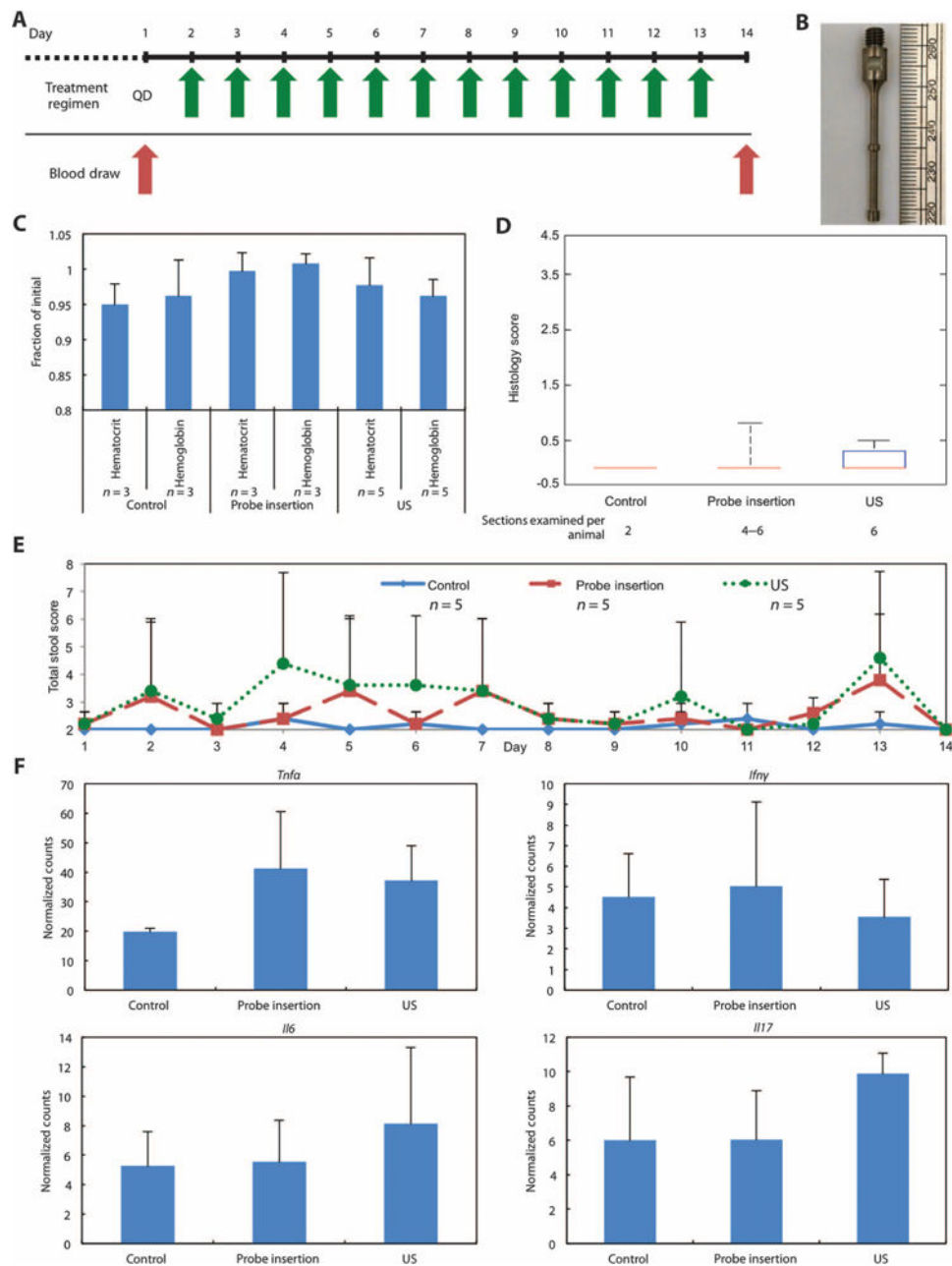


Fig. 4. Effect of rectal ultrasound on blood markers, histology, fecal score, and cytokine expression

(A) Daily ultrasound treatment schedule in healthy pigs in the absence of colitis. (B) The custom-designed ultrasound probe tip with a shaft diameter of 2 mm. The two bumps shown have a diameter of 3 mm and enhance radial ultrasound emission. (C) Hematocrit and hemoglobin normalized to day 1 for healthy animals (control), healthy animals receiving daily probe insertion (probe insertion), and healthy animals receiving daily 40-kHz ultrasound treatment (US). Although five animals were used in each group, some blood samples from days 1 and 14 clotted, resulting in fewer than five values for some groups. (D) Histology scores of tissue sections at day 14. The median, 25th, and 75th percentiles are

shown. The whiskers indicate the most extreme data points. (E) Total fecal score for all three groups over the 14-day period. (F) Cytokine mRNA levels in colonic tissue samples ($n = 4$ biological repeats for all groups). Counts were assessed using the Mouse Inflammatory Panel (NanoString Technologies). Data are normalized across samples using internal positive spike-in controls. Data in (C), (E), and (F) are averages ± 1 SD. Sample sizes indicated are biological replicates.

Author Manuscript

Author Manuscript

Author Manuscript

Author Manuscript

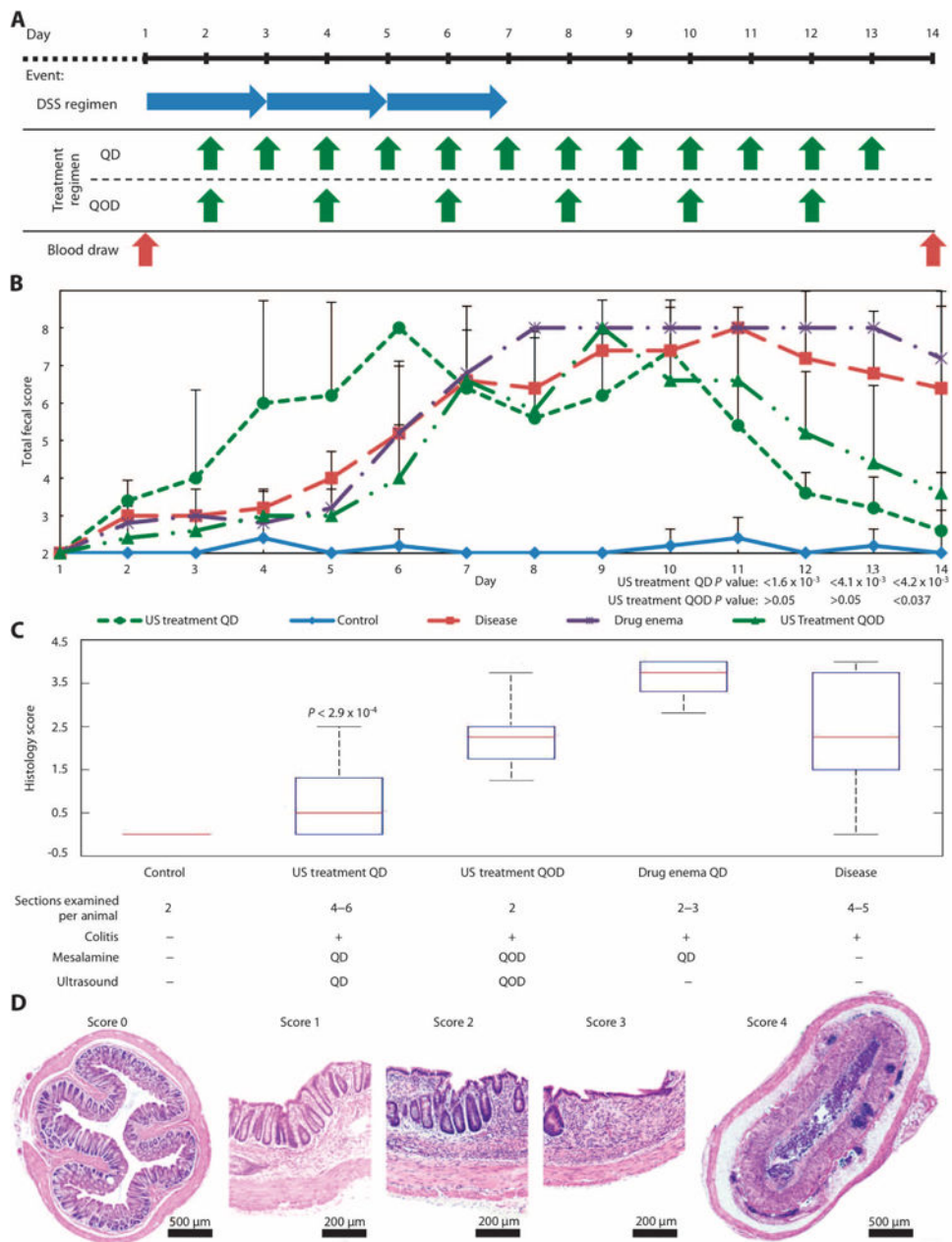


Fig. 5. In vivo radial UMGID of mesalamine in a rodent colitis model

(A) Colitis induction and treatment schedule. DSS was given daily for 7 days to induce acute colitis in mice. Starting on day 2, animals receiving treatment were administered either a mesalamine enema daily (QD), mesalamine with 40-kHz ultrasound QD, or mesalamine with 40-kHz ultrasound every other day (QOD) for 2 weeks. (B) Total fecal score for healthy animals (control) and animals with DSS-induced colitis: receiving no treatment (disease), receiving mesalamine enema daily (drug enema QD), receiving mesalamine enema with ultrasound treatment daily (US treatment QD), and receiving mesalamine enema with ultrasound treatment every other day (US treatment QOD). Data are averages \pm 1 SD ($n = 5$ animals). P values given are for the indicated group receiving ultrasound compared to the

disease and drug enema groups (one-way ANOVA with multiple comparisons). **(C)** Histology scores of colonic tissue sections on day 14 ($n = 5$ animals per treatment group). The median, 25th, and 75th percentiles are shown. The whiskers indicate the most extreme data points. The P value is for US treatment QD compared to all other disease groups (determined by one-way ANOVA with multiple comparisons). **(D)** Histological images of colonic tissue at day 14. Representative images of tissue scored 0 (healthy) to 4.